An investigation into the formations of the internal microstructures of solid dispersions prepared by hot melt extrusion

Fahad Alqahtani[1,2], Peter Belton[3], Bin Zhang[1], Mohammed Al-Sharabi[4], Steven Ross[5], Md Sadeque Hossain Mithu[5], Dennis Douroumis[5], J. Axel Zeitler[4], Sheng Qi[1*]

[1] School of Pharmacy, University of East Anglia, Norwich, NR4 7TJ, UK

[2] College of Pharmacy, Umm Al-Qura University, Makkah, Kingdom of Saudi Arabia

[3] School of Chemistry, University of East Anglia, Norwich, NR4 7TJ, UK

[4] Department of Chemical engineering and Biotechnology, University of Cambridge, Cambridge, CB3 0AS, UK

[5] Faculty of Engineering and Science, University of Greenwich, Kent, ME4 4TB, UK

Corresponding author: Sheng Qi, sheng.qi@uea.ac.uk

Abstract

Hot melt extrusion (HME) is a widely used manufacturing process for pharmaceutical solid dispersions. The complexity of the HME formulations and the number of excipients used in the process are increasing with the advancement of the relevant knowledge. However, one of the areas that are still significantly lacking understanding is the control of internal microstructure of extrudates. Internal microstructure, consisting of voids, in hot melt extruded amorphous solid dispersions is often observed without the causes having been systemically investigated in the literature. In this study, we investigated a range of factors that demonstrated their impacts on the formation of the voids. These include the effect of the types of the materials (i.e. drug, polymer and additive) used in the formulation, the quantity of the drug and the additives used, the key extrusion processing parameters, the type of extruder, and the drying of the raw materials prior to extrusion. The results indicate that the appropriate viscosity and the presence of phase-separated particulates are essential for the formation of the voids. The particulates act as nuclei for the entrapped gas bubbles and the viscosity of the mixture during extrusion governs the collapse/escape of the bubbles. To minimise void formation, the results of this study indicate that slow screw speed, low moisture content of the raw materials, fewer particulates and the addition of lubricants, such as low melting lipid excipients, could be beneficial. This study systematically examines the mechanism of void formation in HME extrudates and generates new strategies that can be used to manage such void formations.

Keywords: Amorphous solid dispersion, hot melt extrusion, void formation, porosity, phase separation, microstructure, controlled drug delivery

Introduction

Hot melt extrusion (HME) has been increasingly used in the large-scale manufacturing and lab research of producing amorphous solid dispersions. In addition to the active pharmaceutical ingredient and the matrix polymer, additives such as plasticizers are often used in HME formulations. Most plasticizers are miscible with the polymer, thus can form a single-phase amorphous dispersion (Solanki et al., 2019, Snejdrova and Dittrich, 2012, Balogh et al., 2014, Maru et al., 2011). However, recently a number of studies reported the use of additives, such as disintegrants and other particulate excipients that form a separate phase to the drug dispersion (Fukuda et al., 2006, Alqahtani et al., 2020, Deng et al., 2013, Krupa et al., 2017, Sadia et al., 2018, Sadia et al., 2016, Crowley et al., 2004). Occasionally, voids were observed in extrudates (Alqahtani et al., 2020, Alshafiee et al., 2019, Fukuda et al., 2006, Martinez-Marcos et al., 2016, Almeida et al., 2011, Crowley et al., 2004). We specifically term such structural features as voids rather than pores because they typically are isolated pockets in the interior of the extrudates and they are not, in most cases, apparent on the surface of the extrudates. The formation of such voids in the extrudates can potentially have significant impact on the physical stability and drug release performance due to their high internal surface area. As an example, in our previous study, a range of additives was used to modulate the drug release rate of HME extrudates containing carbamazepine (CBZ). With 5% w/w loading of these additives, the extrudates exhibited cavitated internal void microstructure (Alqahtani et al., 2020). It was observed that the extrudates with cavitated interiors exhibited accelerated release rates in comparison to the binary polymer-drug solid dispersion (Alqahtani et al., 2020). Therefore, a fuller understanding of why such voids form and how to control them is important to the field of pharmaceutical HME. To the best of our knowledge, there is no study in the literature that has systemically investigated the origin of formation of such internal void structures. The aim of this study was to use a range of model

systems to systemically address this question with a clear focus on examining the factors that could induce the formation of such cavitated internal microstructure.

We hypothesise that voids in the extrudate are formed by bubbles that are held in place when the extrudate solidifies. The bubbles may be formed either by nucleation by residual particles (as the nuclei) in the extruding material or by evaporation of water from water containing particulates. The stability of the bubbles and their survival as cavities will depend on the conditions of extrusion. In this study, we report the detailed investigation into the factors that affect the formation of the voids which leads to our hypothesis of the origin of these voids. The factors studied include the effect of the types of the materials (i.e. drug, polymer and additive) used in the formulation, the quantity of the drug and the additives used, the key extrusion processing parameters, the type of extruder, and the drying of the raw materials prior to extrusion. The results bring new insights into the control strategies of void formation in the pharmaceutical HME extrudates.

Materials and methods

Materials

Carbamazepine (CBZ) and felodipine (FDN) were purchased from Molecula (Darlington, UK). According the melting point (193 °C) and the PXRD diffraction pattern, the crystalline CBZ used for the extrusion experiments is the polymorphic form III (Grzesiak et al., 2003, Caliandro et al., 2013). Hydroxypropyl methylcellulose acetate succinate (HPMCAS-LF) with the substituent ratios of $–CH_3$, $-CH_2CH(CH_3)OH$, $-COCH_3$, and $–COCH_2CH_2COOH$ being 1.87, 0.25, 0.48, and 0.37 average number/glucose ring unit was donated by Shin-Etsu Chemical Co. Ltd. (Tokyo, Japan). Poly(vinyl)caprolactam–poly(vinyl)acetate–poly(ethylene)glycol graft co-polymer (Soluplus®), dimethylaminoethyl methacrylate-co-

polymer (Eudragit® E PO) and sodium starch glycolate (NaSG) were received as generous gifts from BASF (Ludwigshafen, Germany), Evonik (Darmstadt, Germany) and Roquette (Lestrem, France), respectively. Gelucire 50/13, crosscarmellose sodium (CNa) and Crosspovidone (Polyplasdone-XL) (CP) were supplied by Gattefossé (Saint-Priest, France), IMCD UK Ltd (Sutton, UK) and Ashland (Limavady, UK), respectively. Maltodextrin (MD) and α-lactose monohydrate were purchased from (Sigma Aldrich, UK).

Preparation of HME filaments

All formulations listed in **Table 1** (except H-NaSG (EL)) were prepared using a co-rotating twin screw Haake Minilab extruder (Thermo Fisher, Karlsruhe, Germany). The composition of the formulations used for each formulation were summarised in **Table 1**. All HME formulations were extruded at 150 °C with 5 min retention time and at a screw speed at 100 rpm. Clear effects of the process and the addition of NaSG on the void formation were observed for H-NaSG formulation. Therefore H-NaSG is the base formulation of this study and was used to compare the impact of the screw speed and the different scales of extruders on the void formation. When the effects of screw speed on the void formation were studied, 50 and 150 rpm screw speed were also used to extrude H-NaSG formulation. The average extrusion torque value during the retention period was recorded for each experiment. 10 grams of the materials were accurately weighed then premixed using mortar and pestle for 5 minutes. For each extrusion experiment, 7 g of the powder mixture was fed manually into the extruder.

In order to investigate the impact of the extruder on the void formation, a larger scale extruder (EuroLab 16, Thermo Fisher, Darmstadt, Germany) was used to extrude the H-NaSG (EL) formulation at a screw speed of 100 rpm and the detailed processing parameters

are shown in **Table 2**. A circular die of 1.75 mm diameter was used and the extruded strands were guided onto a conveyer belt and collected continuously.

Table 1. Ingredients and hot melt extrusion screw speed of the formulations investigated in this study

Formulation code	**HPMCAS (% w/w)**	**CBZ loading (% w/w)**	**Additives (% w/w)**	**Gelucire 50/13 (% w/w)**
H	100	-	-	-
HG	80	-	-	20
H20	80	20	-	-
HG20	60	20	-	20
H-NaSG	75	20	5 (NaSG)	-
H-NaSG (EL)*	75	20	5(Na SG)	-
HG-NaSG	60	20	5 (NaSG)	15
H30	70	30	-	-
H-NaSG30	65	30	5 (NaSG)	-
H50	50	50	-	-
H-NaSG50	45	50	5 (NaSG)	-
H-CP	75	20	5(CP)	-
HG-CP	60	20	5 (CP)	15
H-CNa	75	20	5 (CNa)	-
HG-CNa	60	20	5 (CNa)	15
H-LM	75	20	5 (LM)	-

HG-LM	60	20	5 (LM)	15
H-MD	75	20	5 (MD)	-
HG-MD	60	20	5 (MD)	15
H-2NaSG	78	20	2 (NaSG)	-
H-7NaSG	73	20	7 (NaSG)	-
Sol-30	70 (Soluplus)	30	-	-
Sol-50	50 (Soluplus)	50	-	-
EPO-30	70 (EPO)	30	-	-
EPO-50	50 (EPO)	50	-	-
H-FDN	75	20 (FDN)	5	-

*This sample prepared on the Eurolab 16 extruder

Table 2: Temperature settings of the extrusion process using Eurolab 16

HME Zones	**1**	**2**	**3**	**4**	**5**	**6**	**7**	**8**	**9**	**10**
°C	25	50	80	130	150	150	150	150	150	150

Thermogravimetric analysis (TGA)

TGA 5500 discovery series (TA Instruments, Newcastle, USA) was used to test the moisture content of the raw materials prior to the extrusion experiments. 5–7 mg of each ingredient were loaded into the instrument and a temperature program of 10 °C/min was used, followed by an isothermal period of 10 min at 105 °C. Trios (TA Instruments, Newcastle, USA) software was used to analyze the acquired results.

Powder X-ray diffraction (PXRD)

XRPD was performed to determine the crystallinity of raw materials, physical mixtures, and extruded formulations using a Thermo ARL Xtra X-ray diffractometer (Thermo Scientific,

Switzerland) operated with CuKα radiation, generator voltage at 45 kV and the current was 40 mA. The angular scan range of 5 – 60° was operated with a (2θ) scan type, 4 s/step scanning rate and the step size was 0.01°.

Differential scanning calorimetry (DSC)

The DSC experiments were carried out using a TA Universal Q2500 Discovery series DSC (TA Instruments, Newcastle, DE, United States) to characterise the raw materials and HME extrudates. A heating rate of 10 °C/min was used from 25 to 210 °C with 50 ml/min nitrogen purge flow. The sample weights in the range of 2-3 mg were used for all samples. TA standard crimped pans and lids were used for all measurements as well as Trios software for analysing the obtained results.

Scanning electron microscopy (SEM)

Zeiss EVO HD15 Scanning Electron Microscope built with Lanthanum Hexaboride LaB6 emitter (Zeiss Microscopy GmbH) and JSM 5900LV Field Emission Scanning Electron Microscope (Jeol Ltd., Japan) equipped with a tungsten hairpin electron gun were used to study the surface microstructure of the formulation extrudates. The samples were coated with gold using a Polaran SC7640 sputter gold coater (Quorum Technologies, city, country) prior to imaging.

X-ray microcomputed tomography (XμCT)

X-ray microcomputed tomography (XμCT) measurements were performed on the different extrudate samples using a Skyscan 1172 instrument (Bruker, Antwerp, Belgium) to investigate their microstructure characteristics and to visualise the distribution of the different ingredients, such as the additive particles, in the extrudates. The XμCT measurements were

conducted using a cone-beam configuration without applying any filter. The 3D imaging of the sample was performed by rotating the sample over 180^{o} with an angular rotation step of 0.4^{o}, and collecting the shadow projected images of the sample at an isotropic voxel resolution of 4.46 μm and an exposure time of 350 ms. 7 frames were averaged per position. Reconstruction of the projected images was then conducted using NRecon software (Bruker, Version: 1.7.4.2) to acquire cross-sectional images of the different extrudate samples. DataViewer software (Bruker, Version: 1.5.3.4) was used to visualise and align the reconstructed images of the samples. The reconstructed images were further analysed using Avizo software (FEI Company, Hillsboro, Oregon, USA, Version: 9.4.0) to create 3D models of the extrudate samples. ImagJ software version 1.52e was also used to measure the pore/void diameter using the reconstructed images of the extrudate samples. For each formulation, two separate samples were tested and the XμCT data were collected and analysed.

In vitro drug release studies

All *in vitro* drug release studies were carried out using the USP rotating basket method (Copley CIS 8000, Copley Scientific) under sink conditions operating at 100 rpm rotation speed with 900 mL of either HCl dissolution medium (pH 1.2) or pH 6.8 phosphate buffer saline (PBS) maintained at 37 ± 0.5 for each test. Two-stage experiments were performed for all dissolution tests to mimic the physiological environment of gastro-intestinal tract. After 2 hours of dissolution in HCl at pH 1.2, the extrudates were removed and the dissolution medium was changed to PBS at pH 6.8. Accurately weighted extrudates containing approximately of 10 mg of CBZ were used in 900 ml medium to ensure sink conditions. 3 ml of the dissolution media were withdrawn from each vessel and filtered through 0.45 μm filters (Minisart Sartorius, Goettingen, Germany) and sampled at predetermined time

intervals. After each sampling, 3 ml of fresh pre-warmed media were replenished to the dissolution vessel. The samples were analysed using a UV–VIS spectrophotometer (PerkinElmer Lamda XLS, USA) at 285 nm. All measurements were performed in triplicate.

Statistical analysis

Statistical analysis was conducted using Graphpad Prism 7 statistical analysis software by the independent Student's T test for comparison of two groups, and one-way ANOVA for multiple groups. All the data are presented as the mean ± SD. *P* values of < 0.05 were considered statistically significant. In all the figures *** is used to indicate $P<0.001$, ** is used to indicate $P<0.01$, and * is used to indicate $P<0.05$.

Results and discussion

The formation of the interior void structure in HME extrudates

As seen in **Figure 1**, except the H-CP and its placebo extrudates, the rest of the formulations all exhibit an interior with voids. From the previous study, it was confirmed by the DSC results that CP is miscible with HPMCAS and CBZ (with 20% drug loading) and forms a single-phase solid dispersion after HME (Alqahtani et al., 2020). As seen in **Figure 1**, the phase separated additive particles can be identified in both placebo and drug loaded extrudates containing CNa, NaSG, LM and MD. However, it is obvious that without the addition of CBZ, the placebo extrudates are either void-free or have much lower density and smaller sized voids than the CBZ loaded extrudates.

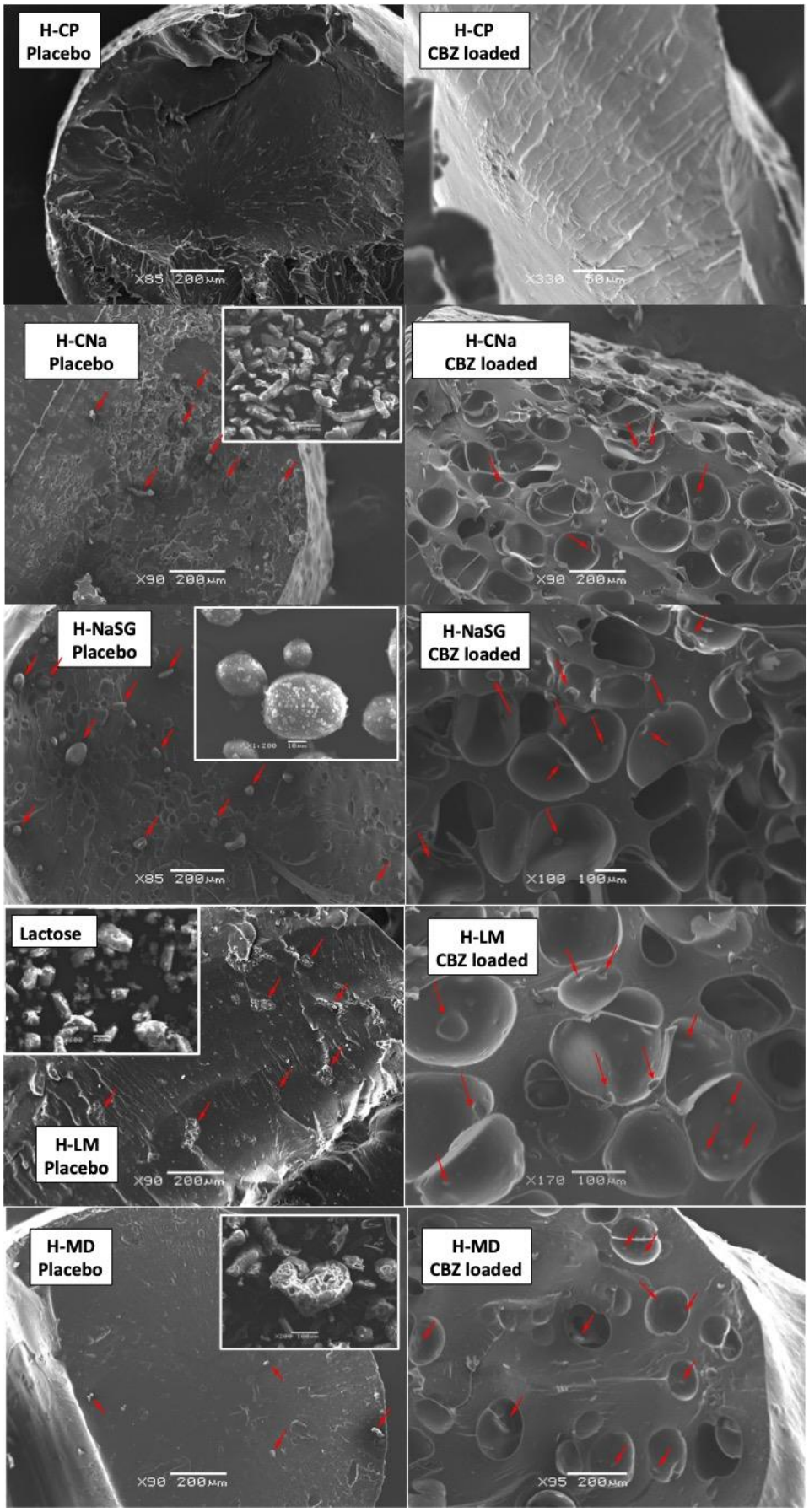
H-CP
Placebo
X85 200µm
H-CP
CBZ loaded
X330 50µm
H-CNa
Placebo
X90 200µm
H-CNa
CBZ loaded
X90 200µm
H-NaSG
Placebo
X85 200µm
H-NaSG
CBZ loaded
X100 100µm
Lactose
H-LM
Placebo
X90 200µm
H-LM
CBZ loaded
X170 100µm
H-MD
Placebo
X90 200µm
H-MD
CBZ loaded
X95 200µm

Figure 1. SEM images of the cross-sections of the samples showing the effects of additives on the void formation in the interior of the extrudates. (The additive particles are highlighted by the red arrows in each image)

XμCT allows the detection of the additive particles when they contain either Na or Ca, which have higher atomic mass than the atoms of HPMCAS and the drug. The colour coding is used to visualise the additive particles in the extrudates (individual images with enhanced resolution can be found in the Supplementary Information). As seen in **Figure 2**, the atomically denser additive particles can be seen as the red dots showing in the XμCT images. This is particularly evident in the case of H-NaSG and H-CNa. The XμCT analysis of the extrudates confirms that the additive particles are mostly located at the surface of the voids. The voids often have a distorted spherical shape. Both SEM and XμCT results confirm that the voids are not interconnected, but that the individual voids are present in isolation. These results indicate that the co-existence of the drug and the additives are essential for the formation of the voids inside the extrudates. The fact that the single-phase dispersion H-CP extrudates are void-free indicates that the additive particles play an important role in the formation of the voids. We hypothesis that the possible factors involved in void creation are moisture, particulate additives, drug, viscosity, extruder conditions. In the following sections we investigate these factors systematically.

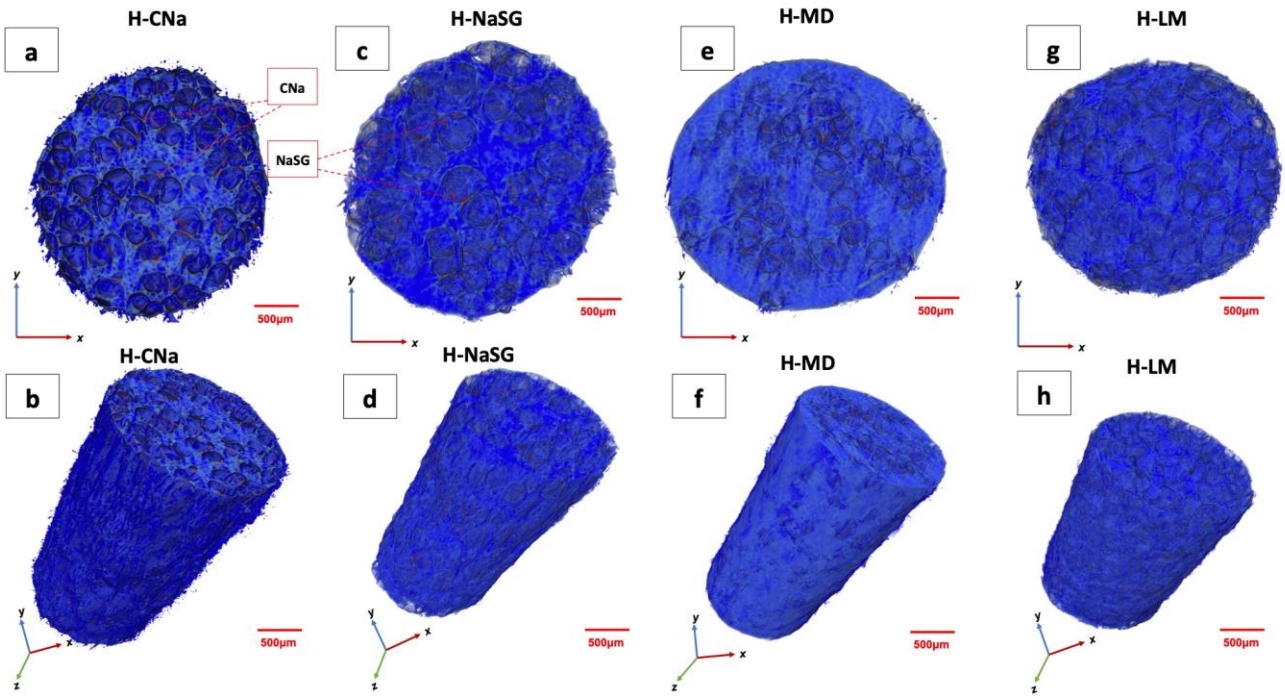

Figure 2. Cross-sections (top) and 3D visualisation (bottom) of the XμCT images of the extrudates with additives. The matrix of the polymer-based extrudates are in blue and the red dots embedded in the blue matrices of H-CNa and H-NaSG are the CNa and NaSG particles. The higher atomic density of sodium in CNa and NaSG than the polymer matrices increased the contrast and allowed the identification of these particles in (a)-(d). (Enlarged individual images can be found in the Supplementary Information)

Effect of moisture contents of the raw materials

Both HPMCAS and CBZ contained less than 1% (w/w) moisture. The moisture contents of the additives were measured using TGA and the results are summarised in **Figure 3a**. The additives all carried 3-7.5% (w/w) moisture prior to extrusion, thus it is reasonable to hypothesis that the moisture contents of the raw material may have an effect on the void formation. As the extruder is well ventilated, any volatile solvent from the feed powder mix should be easily eliminated during the heating and mixing process of the extrusion, unless the molten mass in the extruder was too viscous to allow the escape of the entrapped gas. This is

supported that the data shown in **Figure 3b and 3c** indicating no clear correlation between the amount of moisture content with the void diameter. This indicates that the moisture content of the particles of the additives is not the sole cause of the formation of the voids. Nevertheless, it is clear that in order to reduce the number and density of voids, reducing the initial moisture in the raw materials may be desirable. When the raw materials of the additives were dried for 6 hours at 105 °C, both void size and void density in the extrudates were dramatically reduced, as seen in **Figure 4**.

Therefore, we hypothesise that during the extrusion process, the particles of the additives are the source of water that forms vapour which in turn results in the voids that can be detected in the finished extrudates. Since dry particles produce some voids it is also likely that they act as nuclei for dissolved air. These gas bubbles are entrapped, i.e. they cannot escape, due to the high viscosity of the mix and thus remain as voids that can be observed in the extrudates after cooling. Therefore, the effects of viscosity of the formulations were investigated in the following sections.

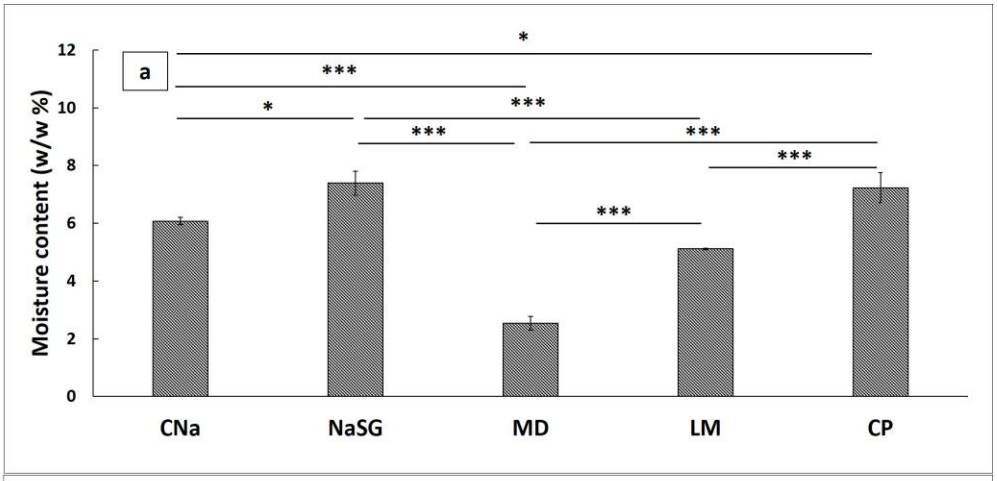
a
Moisture content (w/w %)
0
2
4
6
8
10
12
*
***
*
***
***
***
***
***
CNa
NaSG
MD
LM
CP

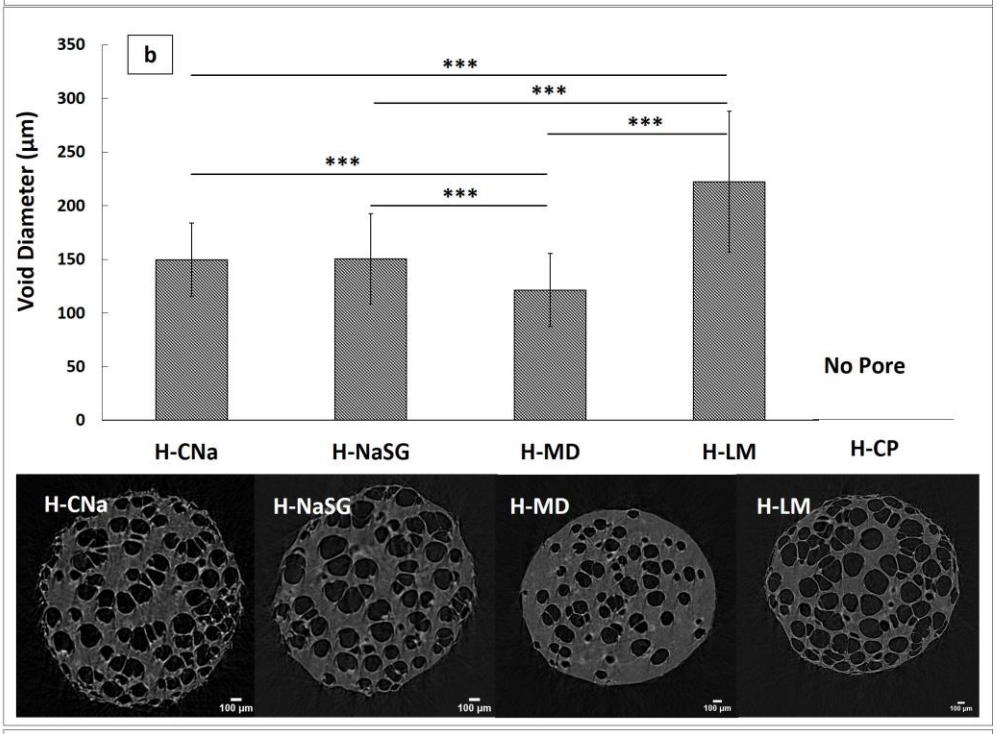
b
Void Diameter (µm)
0
50
100
150
200
250
300
350
***
***
***
***
***
No Pore
H-CNa
H-NaSG
H-MD
H-LM
H-CP
H-CNa
H-NaSG
H-MD
H-LM
100 µm

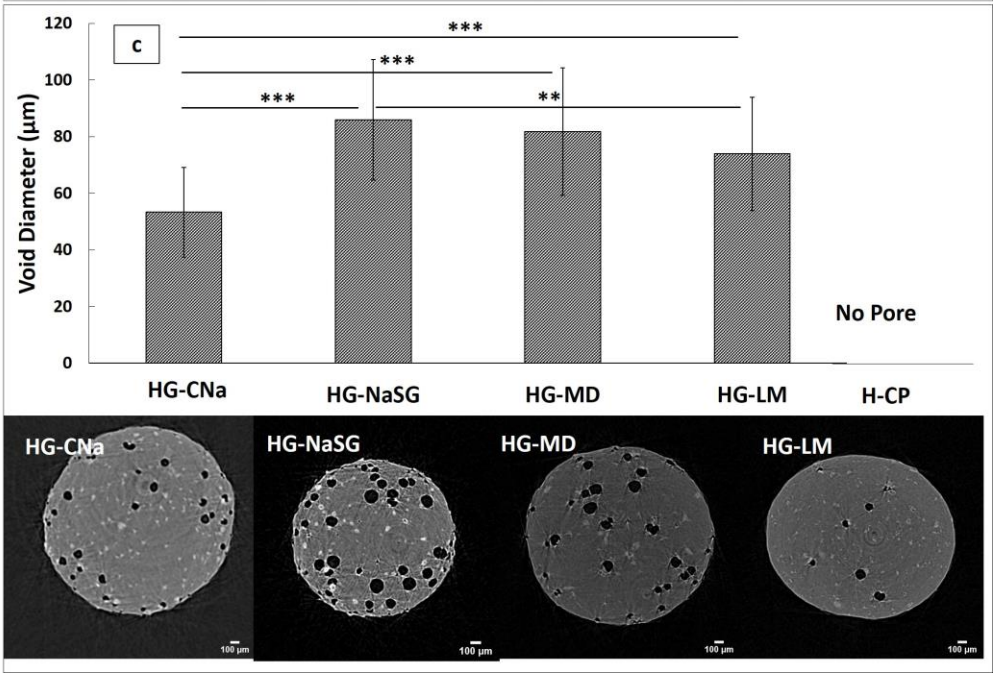
c
Void Diameter (µm)
0
20
40
60
80
100
120
***
***
***
**
No Pore
HG-CNa
HG-NaSG
HG-MD
HG-LM
H-CP
HG-CNa
HG-NaSG
HG-MD
HG-LM
100 µm

Figure 3. Correlation between the void diameter and the moisture contents in the raw materials. (a) Moisture contents of raw materials measured by TGA; (b) pore diameters of the HME extrudates with additives; (c) pore diameters of HME extrudates with Gelucire 50/13 and the additives. The pore diameters in (b) and (c) were measured using the XμCT data. Representative XμCT images of the cross-section of each formulation are shown at the bottom panels of (b) and (c). As the extrudates of H-CP and HG-CP are completely void-free, no XμCT images are shown here. The data are represented as the mean ± SD, n = 2 (***P<0.001, ** P<0.01, and *P<0.05).

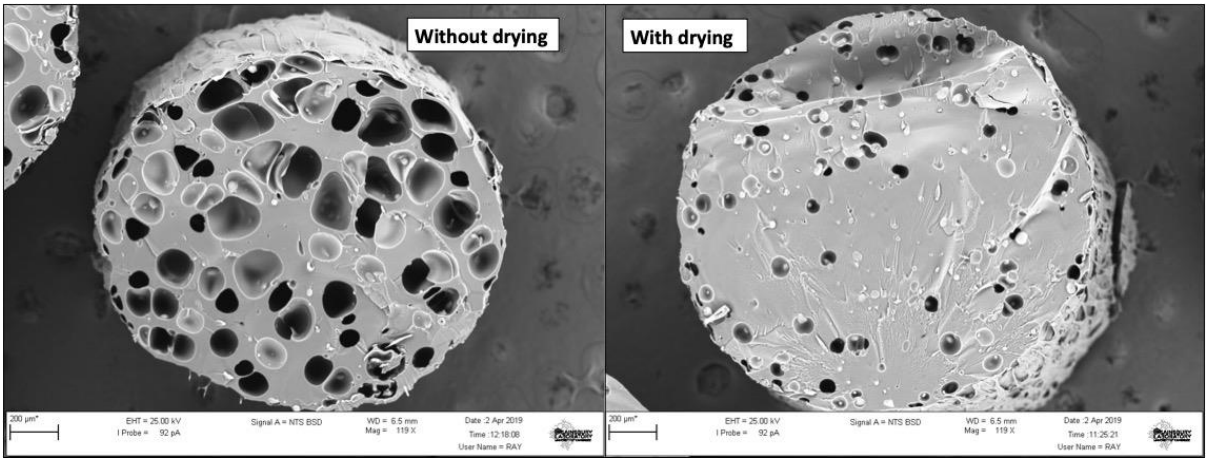

Figure 4. SEM images of the cross-sections showing the effect of drying of the raw materials on the formations of the voids.

Effect of viscosity

During the HME process, the recorded torque value is a direct reflection of the viscoelastic properties of the material being processed in the extruder. **Figure 5** shows the recorded torque values of all the formulations with and without drug (**Figure 5a**) and with and without Gelucire 50/13 (**Figure 5b**) in the formulations. The binary mixture of HPMCAS and 20% CBZ (H20), the drug is completely solubilised in the polymer and forms an amorphous solid dispersion (Alqahtani et al., 2020). With a lower glass transition temperature (T_g) of 56 °C

compared to HPMCAS (with a T_g of approximately 120 °C), CBZ exhibited a clear plasticisation effect on the polymer and reduce the viscosity of the mixture in the extruder which led to the significant reduction in torque required for extrusion in comparison to HPMCAS alone. As seen in **Figure 6a-c**, the binary extrudates without the particulate additives, with increasing the drug load from 20% to 50% w/w, the density of the voids increases. This indicates that reduced viscosity to a certain level could potentially favour the formation of the voids. In general terms, if the air bubbles were entrapped in a viscous liquid, increased viscosity of the liquid would make the escape of the air bubbles (using velocity of the bubble as the measure) more difficult (slower velocity of movement in the liquid) according to the Stokes formula (Smirnov and Berry, 2015, Landau and Lifshitz, 1987). However in the case of this study, the results indicate that a balance is required: if the viscosity is too high bubbles won't grow and if it is too low bubbles will grow to burst or escape to the surface. Since both polymer type and drug loading may affect viscosity of the molten mixture in the extruder, both may affect cavity formation by changing viscosity. This result agrees well with the similar void-forming phenomena reported in the literature (Alshafiee et al., 2019, Martinez-Marcos et al., 2016, Fukuda et al., 2006).

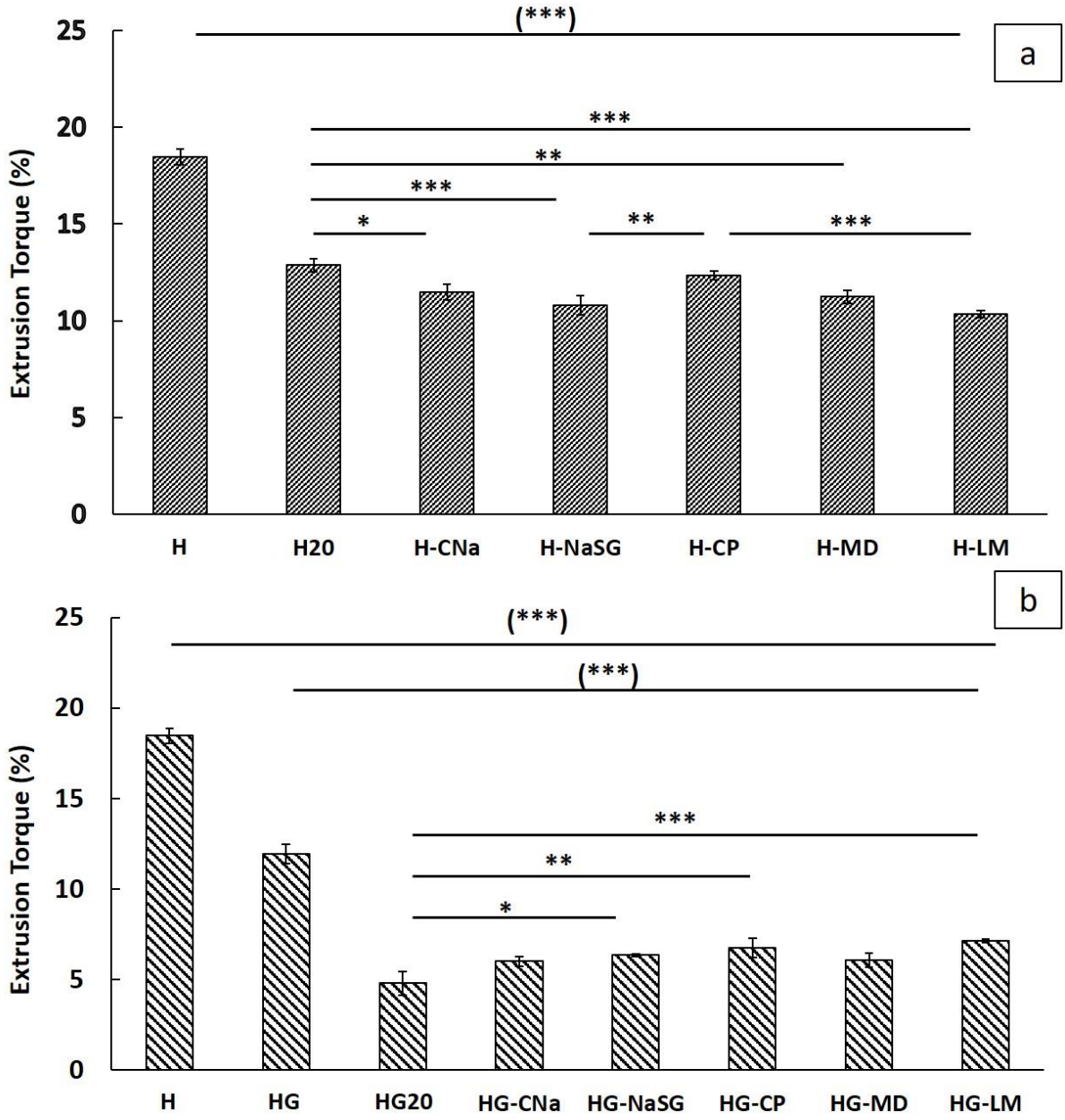

Figure 5. The average torque values (%) recorded during the hot melt extrusion process of the formulations (a) without and (b) with Gelucire 50/13. The data are represented as the mean ± SD, n = 3 (***P<0.001, ** P<0.01, *P<0.05 and (***) indicates that the torque value is statistically significantly (with a P<0.001) different from the rest of the formulations in the group).

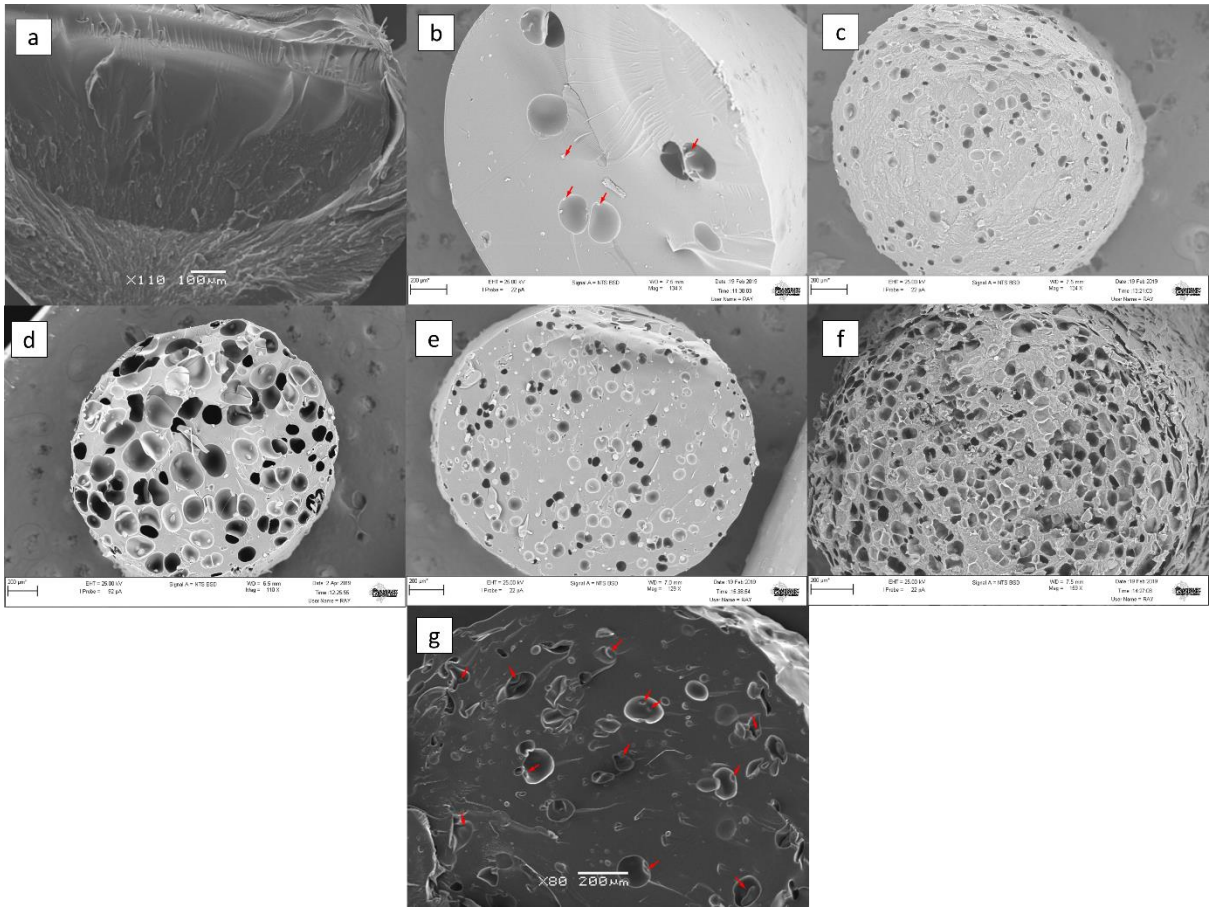

Figure 6. SEM images of the cross-sections showing the combination effect of drug loading and addition of the additive on the formation of the voids. (a) H20; (b) H30; (c) H50; (d) H-NaSG; (e) H-NaSG30; (f) H-NaSG50; g) H-FDN.

In addition to the differences observed in the numbers of voids in the extrudates with different drug loadings, the diameters of the extrudates also increases with increasing the drug content and the screw speed, as shown in **Figure 7**. The larger diameter of the extrudates with higher drug contents (both with and without the particulate additives) may be a result of the higher numbers of voids than the ones with lower drug loading systems (**Figure 7a**). At the extruder die orifice, the sudden pressure drop allows the gas in the voids to expand in volume. This leads to the expansion of the diameter (often referred as "die swell"). Higher screw speed provides higher shear stress and internal pressure in the extruder

which leads to more die swell. However this did not lead to significant difference in the diameter of the extrudates produced by different screw speeds, as observed in **Figure 7b**.

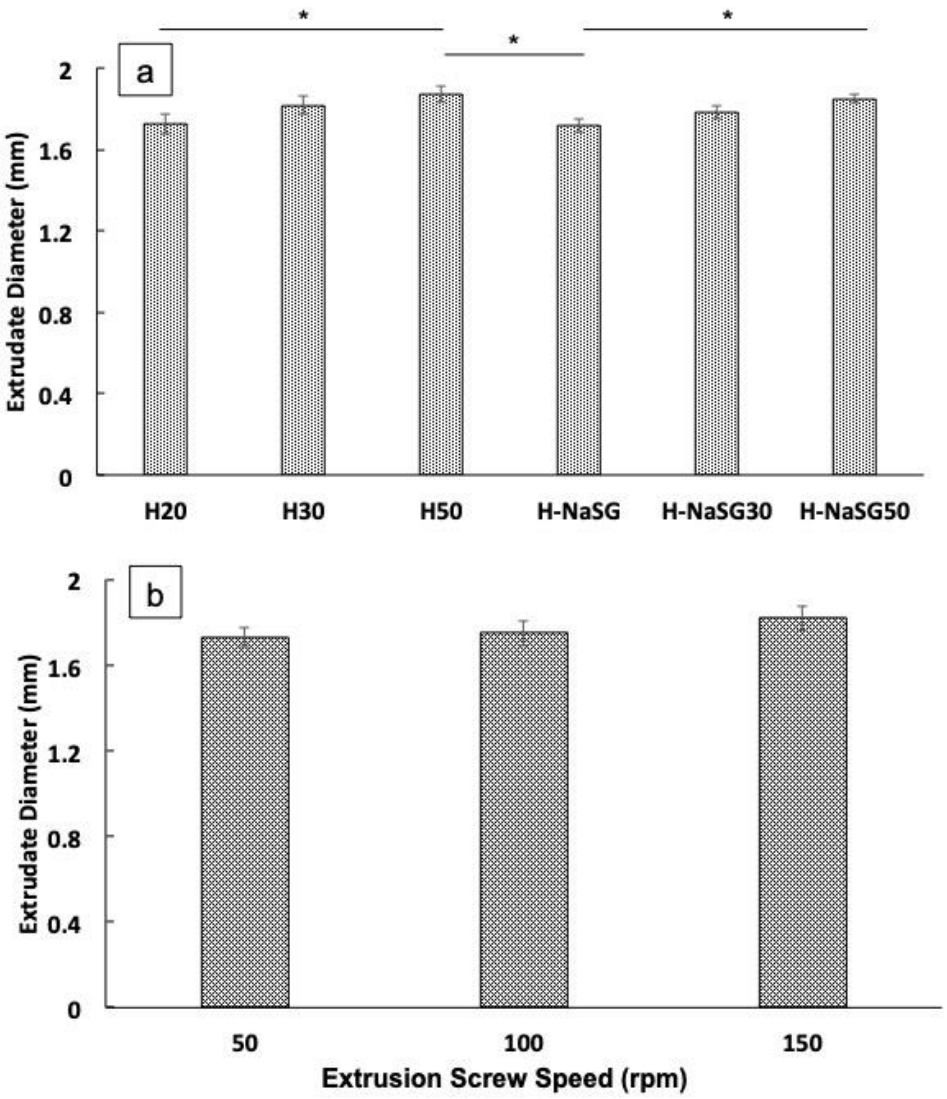

Figure 7. The summaries of the extrudates diameters: (a) The extrudates containing 20, 30, 50 % w/w CBZ loaded in HPMCAS (H20, H30, H50) and 20, 30, 50 %w/w CBZ loaded in HPMCAS with 5 %w/w NaSG (H-NaSG, H-NaSG30, H-NaSG50); (b) HPMCAS-CBZ binary extrudates diameters produced using screw speeds of 50, 100 and 150 rpm. The data are represented as the mean ± SD, n = 3 (*P<0.05).

It is noted that very few small particles can be seen in the interior of the extrudates with 30% drug loading. As seen in **Figure 8**, the DSC results of the 30% drug loaded extrudates show a

T_g at approximately at 65 °C which is lower than the theoretical calculated T_g of the binary mixture according to Gordon-Taylor equation; whereas the T_g of the 50% drug loaded extrudates (H50) is in the same region of the amorphous CBZ, which is around 56 °C, indicating the presence of a significant amount of amorphous drug. The PXRD results confirm that 30% drug loaded extrudates are largely amorphous and 50% drug loaded extrudates contain a significant amount of crystalline CBZ. These results indicate that 30% drug loading approaches the saturation of the solubility of the drug in HPMCAS and 50% binary extrudates are supersaturated with crystalline drug. In a way similar to the dried phase separated additives, these un-dissolved drug particles could act as the nuclei of the gas bubbles and facilitate the formation of the voids. Therefore, in the case of 50% drug loaded binary extrudates, viscosity is not the sole factor causing the voids.

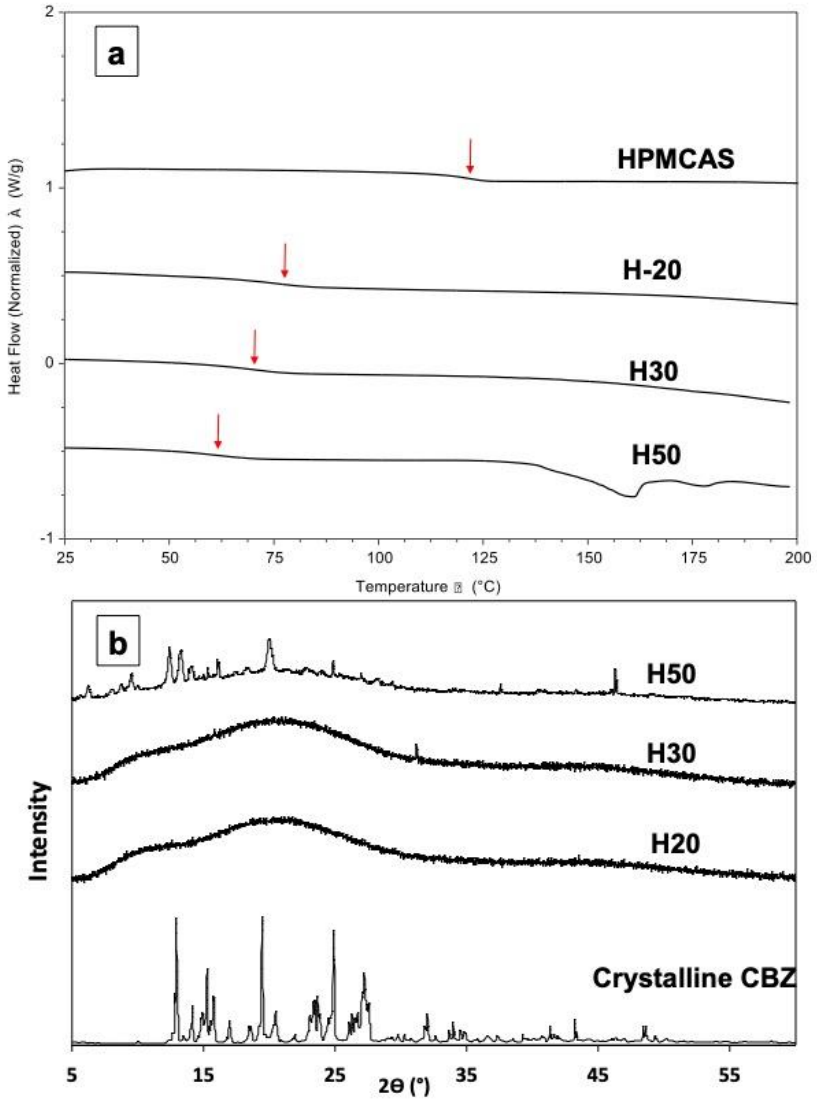

Figure 8. (a) DSC and (b) PXRD results of the binary extrudates with the drug loading ranging from 20-50% w/w.

As seen in **Figure 5a**, the addition of 5% (w/w) particulate additives of CNa, NaSG, LM, and MD resulted in further significant reductions of the viscosity and subsequently the torque values of the extrusion process in comparison to the binary extrudates of H20. This was not the case for H-CP. As discussed earlier, H-CP forms a single-phase dispersion because CP is miscible with HPMCAS and CBZ at the proportion used in the formulation. CP was homogenously mixed and formed a single-phase molecular dispersion with HPMCAS and

CBZ. We speculate that any moisture carried by the additive would be homogeneously distributed and there are no nucleating sites for bubble formation. In the case of the other phase-separate particulate additives, water is concentrated locally in the particle and the release of a relatively large amount in a small region causes bubble formation. When the moisture turns to steam, it generates a significant volume of gas around each particle (approximately 1 cm^3 of gas per g of matrix depending on the details of temperature and pressure).

A significant further reduction of the torque was observed when Gelucire 50/13 was added to the binary and ternary formulations, as shown in **Figure 5b**. This may contribute to the remarked reductions on both the void size and void density seen in **Figure 3c**. Gelucire 50/13 is a semi-crystalline lipid-based additive that is not miscible with HPMCAS. This is confirmed by the measureable melting of Gelucire in the DSC results of the extrudates (Alqahtani et al., 2020). At the extrusion temperature used in this study, the melt viscosities of fats and lipids are typically much lower in comparison to polymers, such as HPMCAS. As the molten Gelucire 50/13 is phase separated from HPMCAS, during the thermal extrusion, Gelucire acts as a 'lubricant' of the molten mixture and reduces the overall melt viscosity of the system in the extrusion. This facilitates the escape/collapse of entrapped gas bubbles and leads to fewer and smaller voids. The possibility of molten Gelucire coating the additive particles may also reduce the number of the nucleus sites of the gas bubbles which may contributed to the significantly fewer voids with smaller diameters in the Gelucire containing extrudates seen in **Figure 3c**.

With the model particulate additives, 5% NaSG (w/w), increasing the drug loading should lead to reduced viscosity during extrusion due to the drug's plasticisation effect on

HPMCAS. We observed a reduction of the size of the voids, but this coincided with increased density of the voids (**Figure 6e**). This could be attributed to the break-up of each large void into a number of small satellite voids when the viscosity is low (but still sufficient to entrap the bubbles). Therefore, the results suggest that there is a critical minimal viscosity of the mixture that above this viscosity the mixture would be able to retain the bubbles and allow the shape deformation, but without collapse of the bubble.

The H-NaSG50 extrudates (with 5% NaSG and 50% drug load) are a much more complex case. The 50% mixture is saturated since 30% drug is the solubility limit. Hence the viscosity of the mixture should be similar to that of the 30% mixture which can form voids. However there are more particles in the 50% mixture due to un-dissolved drug. Nucleation from these particles results in more gas bubbles formed hence the 50% extrudates show a larger number of voids.

In order to eliminate the possibility that the formation of voids in the extrudates is drug specific, another model drug, felodipine (FND), that has a slightly lower T_g than CBZ, was tested. As seen in **Figure 6g**, interior voids in H-FDN extrudates are still clearly visible. Solid particulates can be seen at the interface of the voids. This confirms that the void formation is not drug specific and the presence of phase separated solid particulates is essential for void-forming.

To further confirm that the void-forming is not polymer specific and to prove that the viscosity of the mixture in the extruder is one of the key factors determining the formation of the voids, two different polymers with different reported melt viscosity were used. Binary extrudates of CBZ with Soluplus and Eudragit® E PO, two widely used HME polymers, were

prepared without NaSG. At the HME temperature used in this study (150 ºC) the complex viscosity measured is in the order of Eudragit® E PO ($10^{3.1}$ Pa.s) ≈ Soluplus ($10^{3.8}$ Pa.s) <HPMCAS ($10^{5.2}$ Pa.s) (Parikh et al., 2016, Meena et al., 2016, Gupta et al., 2016). The extrudate diameters of H30 ad H50 are significantly higher than the Eudragit® E PO and Soluplus based extrudates (data shown in Supplementary Information). As seen in **Figure 9**, both Sol-30 and EPO-30 show either no void or very low numbers of small voids compared to the ones observed in H30 extrudates, despite the clear observation of the presence of recrystallized drug particles (highlighted by the red arrow). The DSC and PXRD data shown in **Figure 10** confirmed these being recrystallized drug particles. From the melting point and the PXRD diffraction patterns, it is clear that the recrystallized drug particles are in different polymorphic form (form I) from the starting material which is CBZ form III (Grzesiak et al., 2003, Caliandro et al., 2013). This indicates that 30 and 50% drug loadings formed supersaturated solid dispersions for both Soluplus and Eudragit EPO. This confirms that a sufficient level of viscosity is important for the void formation and that when the viscosity is below the critical minimal viscosity void formation can be eliminated altogether even the presence of solid particles.

With increasing the drug loading to 50%, a significant amount of recrystallized drug particles can be observed in all formulations. Consequently, voids are observed in both H50 and EPO-50 extrudates. However, it is interesting to see that the Sol-50 shows no voids, despite the recrystallized drug particles being visible. We speculate that this may be due to the low interfacial tension between Soluplus and the drug particles. Soluplus is a surface-active polymer that may be easier to be spread and ‘wet’ the surface of the drug particles. However, this is speculative and further experiments are required which are out of the scope of this study.

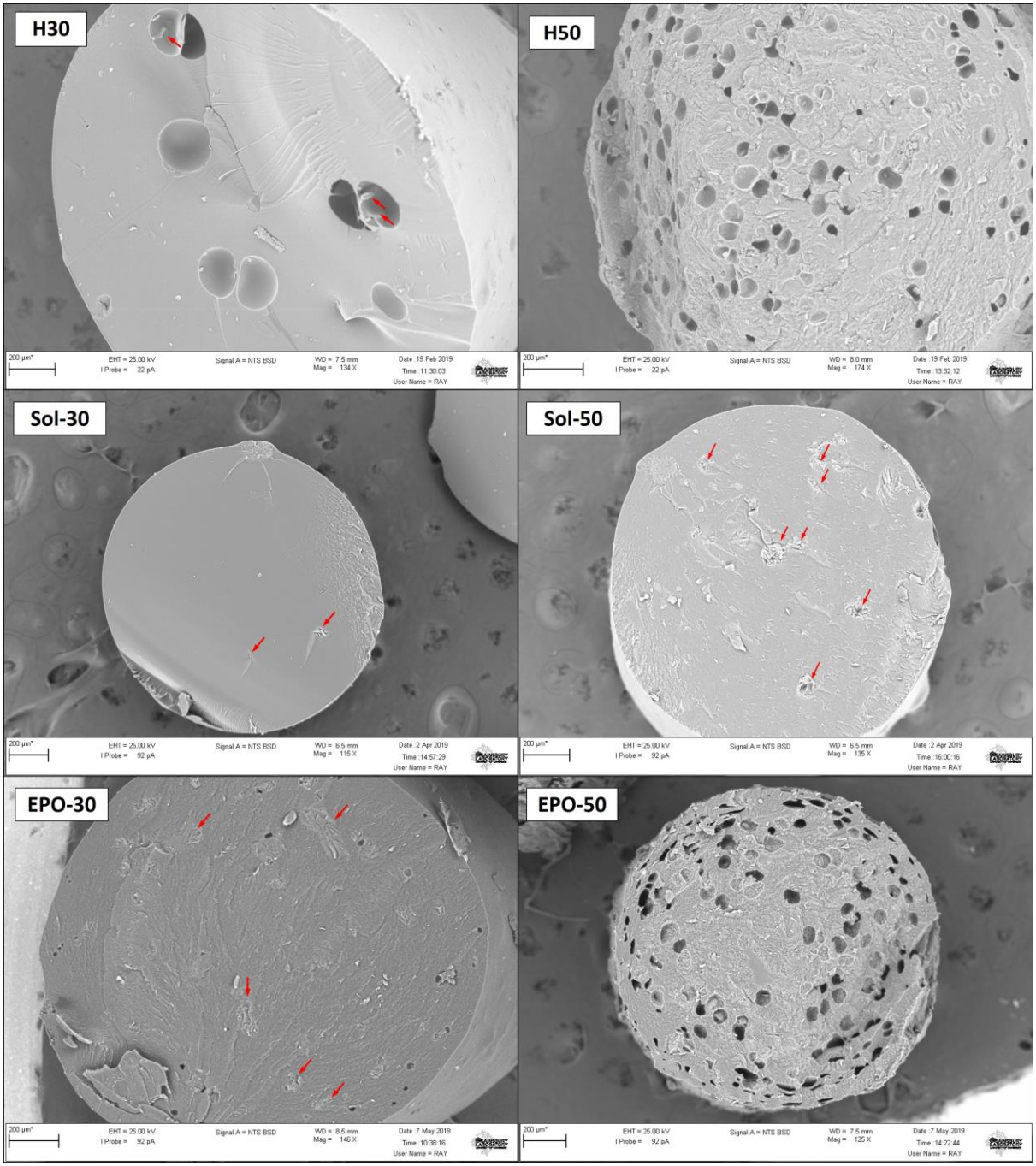

Figure 9. SEM images of the cross-sections of the extrudates showing the effect of matrix polymer type and drug loading on the void formation. All formulations were additive-free (red arrows indicate the presence of possible recrystallized drug particles).

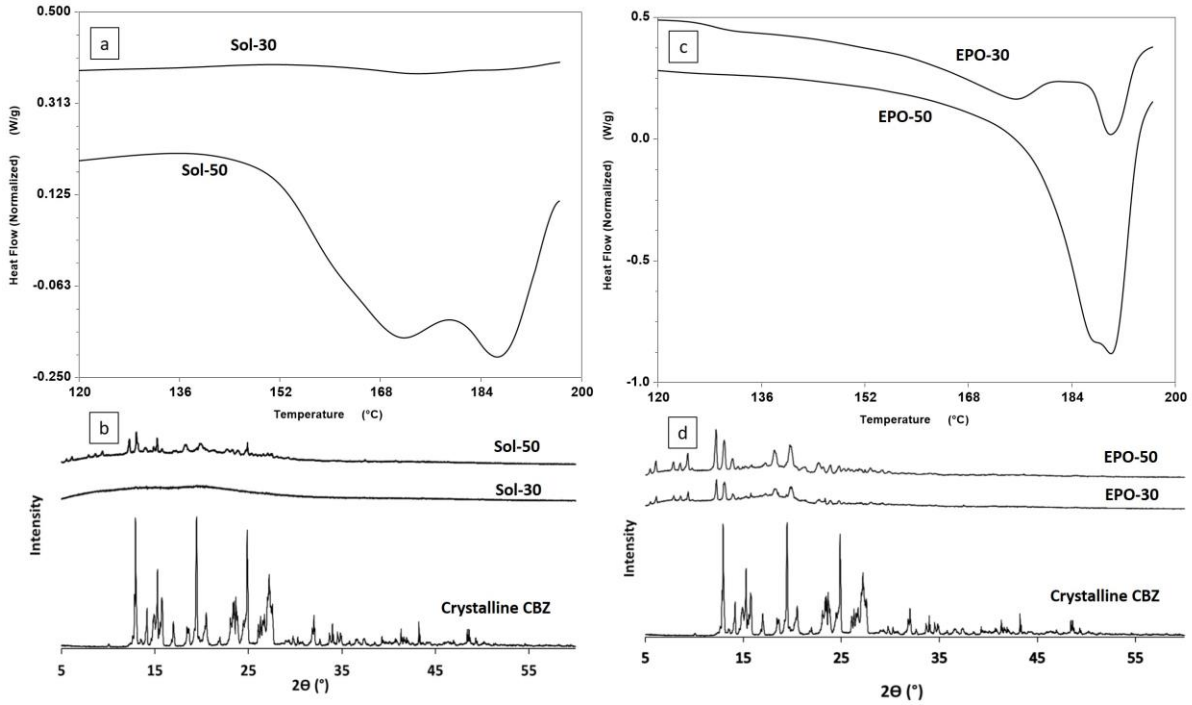

Figure 10. DSC (a and c) and PXRD (b and d) data of Sol-30, Sol-50 and EPO-30 and EPO-50.

Effect of process parameters

As the formation of the voids is a result of the extrusion process, it is important to examine the effect of extrusion operation on the void formation. The bubble entrapment and collapse in the viscous polymer-drug mixture during the extrusion can be affected by the external perturbations experienced by the bubbles. Similar to complex multi-phase fluid flow, such sources of perturbations include the shock generated by the collapse of a neighbour bubble, shape deformation caused by the large fluctuations of longitudinal and transverse velocity of the mixture that the bubbles are embedded in during the high shear movement of the extrusion, and uneven shear experienced by the mixture closer to the surface and beneath the surface of the rotating screws (Hann et al., 2018). Based on this, we hypothesise that different levels of surface shear would influence the void formation. On the basis of this hypothesis, we employed a range of screw speeds to investigate the effect of the combination of the flow velocity and shear on the formation of voids. Unfortunately, for a manufacturing process such

as HME, it is impossible to separately investigate a single factor in isolation, as increasing shear would also lead to a change in fluid velocity. Nevertheless, it should provide new insights into the control strategy of the void formation.

As seen in **Figure 11**, the screw speeds used during HME show a clear effect on the void diameter and the void density. At slower screw speeds, fewer voids were generated (**Figure 11a**). These voids were much smaller in diameter in comparison to the voids that were observed in the extrudates manufactured at 100 rpm screw speed. It is also noted that most of the well-defined voids (30-50 µm in diameter) are mainly located close to the edge of the extrudates. The small voids (10-20 µm in diameter) were scattered across the interior of the extrudates often showed a furrow tail. All these furrows are oriented in the same direction, which could well coincide with the rotation direction of the screw. Increasing the screw speed from 100 to 150 rpm resulted in a reduction of the void diameter by about half and an approximate 200% increase of the void density (**Figure 11c**). If the viscosity of the mixture was sufficient to hold the bubbles, the faster screw rotation could cause the deformation of the void shape and the breakage of a large void into smaller voids. This could explain the observed increased density and reduced void size. The differences between the mean void diameters of the extrudates processed by the three screw speeds are significantly different (**Figure 11e**), indicating the screw speed has a profound impact on the void formation. The results suggest that a slow screw speed needs to be selected to avoid void formation during extrusion.

Often lab scale bench top extruders are built with much shorter screws in comparison to industrial scale extruders. Therefore, the same formulation (H-NaSG) was prepared using a larger extruder (H-NaSG(EL)), EuroLab 16, to ensure that void formation is not an artefact of

the small lab scale extruder. As seen in **Figure 11d**, although the overall diameters of the extrudates are larger than the extrudates produced by the bench top extruder, the void diameters are not statistically significantly different from the ones produced by the small bench top extruder (**Figure 11f**). The difference in the diameter of the extrudates is due to the different size of die used on the large and bench top extruder. This result confirms the porosity is intrinsic to the formulation and the process, but not the scale of the extrusion instrument.

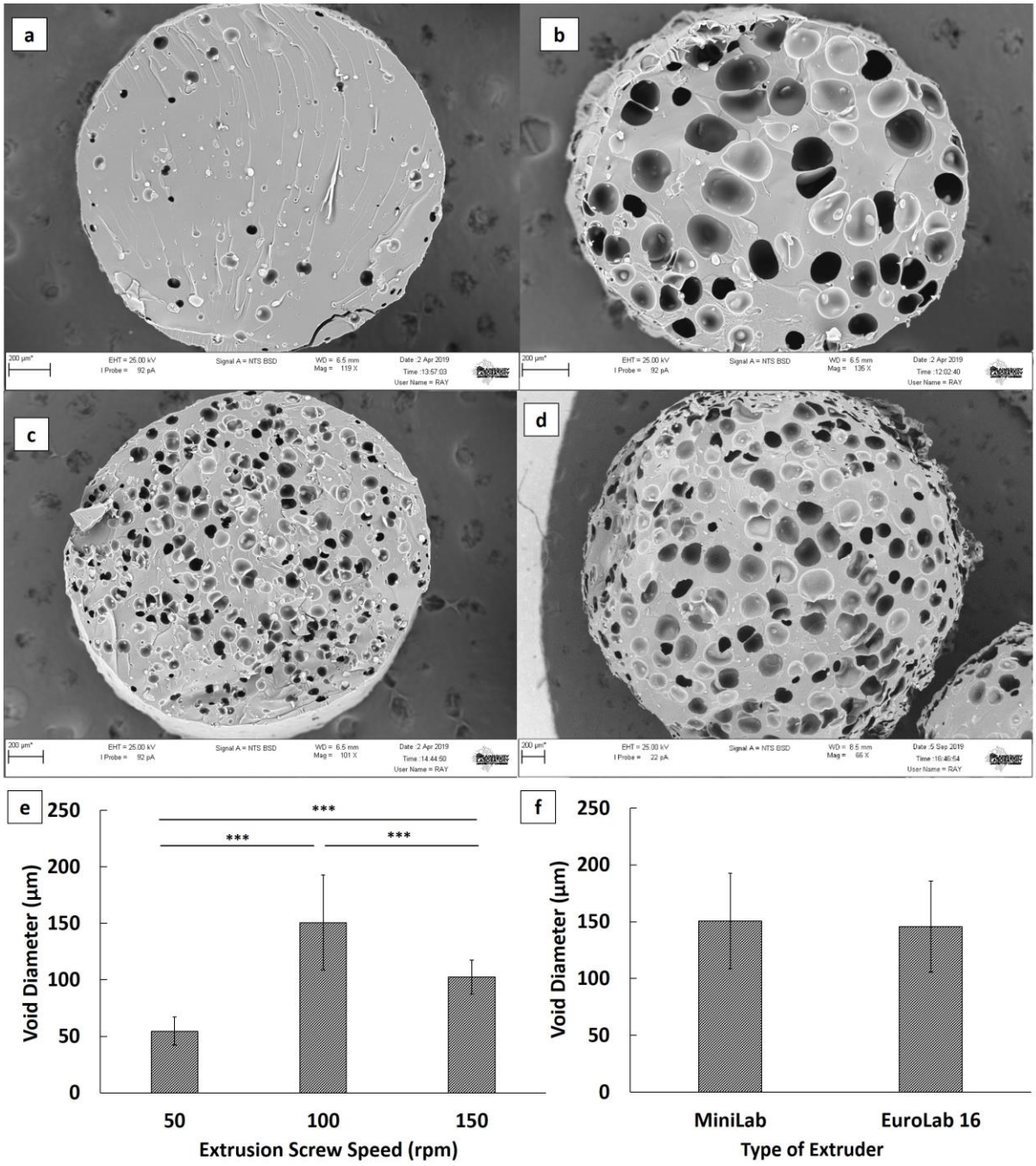

Figure 11. SEM images of the cross-sections of the interior structures of H-NaSG extrudates produced using a) 50 rpm; b) 100 rpm; c) 150 rpm screw speed on a Mini-lab twin screw extruder and d) H-NaSG (EL) produced by a Eurolab-16 Extruder at 100 rpm screw speed. The data are represented as the mean ± SD, n = 3 (***P<0.001).

Effect of porosity on drug release

If the extrudates were to be used as the dosage form (such as strands or short pellets), it is important to understand the impact of the interior voids on the drug release behaviour of the formulations. As seen in **Figure 12**, whatever the method used to induce void formation (either by changing the loading of the particulate additives, or the drug loading or the screw speed), a clear trend of higher relative void volume leading to a faster dissolution is observed. Drug loading shows the most profound impact on the drug release rate with shortening the T_{50} from 15 hours to 3.6 hours when changing the drug load from 20% to 50% (w/w). As seen in **Figure 6**, the extrudates with 50% drug loading have almost a honeycomb structure. Due to there high relative void volume, the material density per unit volume of H50 is significantly lower than the ones of H20. This may explain the rapid dissolution data. The changes in release rates due to changes in screw speed and NaSG loading were less dramatic than that the effects of changes in drug loading reflecting the smaller changes in relative void volume.

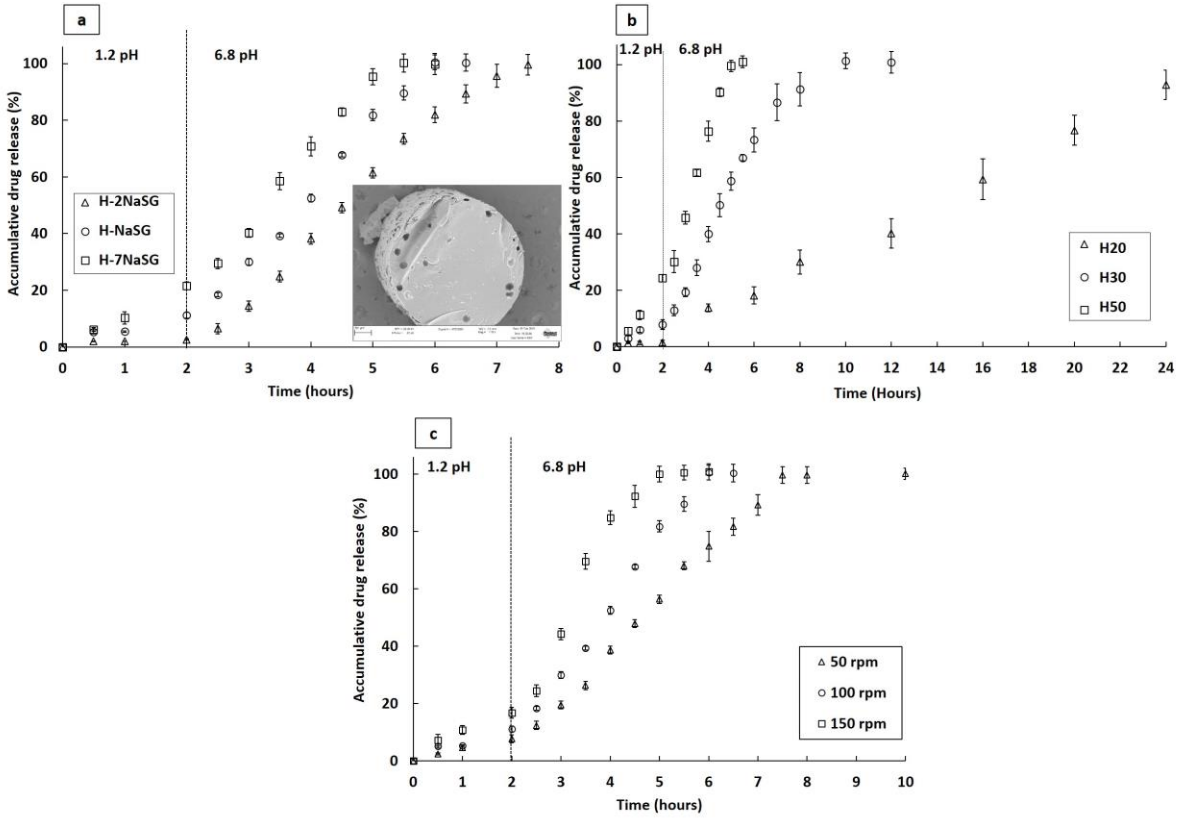

Figure 12. The in vitro drug release (0-2 hours in pH 1.2 simulated gastric pH followed by replacement of pH 6.8 PBS as the dissolution media) data of a) extrudates with a loading of NaSG ranging from 2-7% w/w (with the insert being the SEM images of 2% NaSG extrudates with a lower void density than others) (H-2NaSG, H-NaSG, H-7NaSG); b) binary extrudates with a drug loading ranging from 20-50% w/w (H20, H30, H50); c) H-NaSG extrudates processed using screw speed ranging from 50-150 rpm.

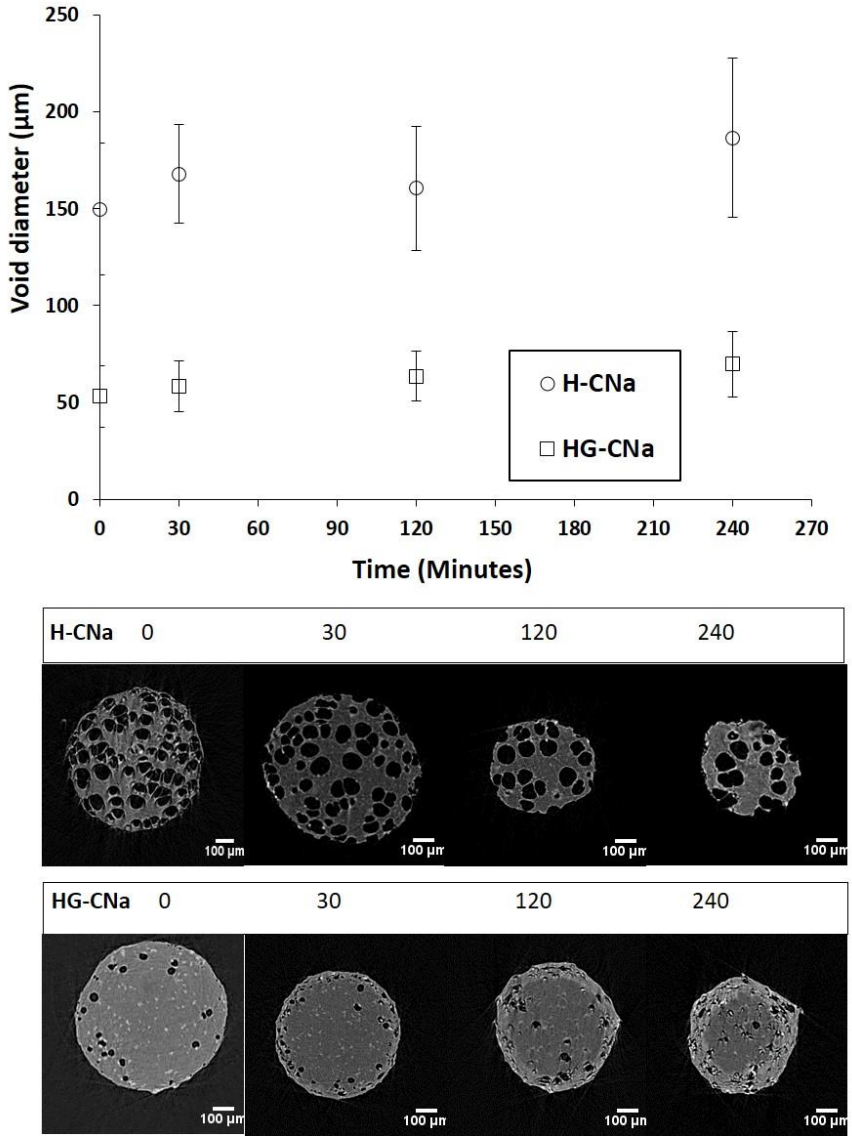

Figure 13. Void diameter change of H-CNa and HG-CNa during the dissolution process with the bottom panel showing the representative reconstructed cross-section images of the XμCT

data of the H-CNa and HG-CNa extrudates taken at different time intervals during the dissolution test.

In order to further confirm the role of the voids playing in facilitating the dissolution process, the void size and distribution were monitored during the dissolution process. As seen in **Figure 13**, despite with or without Gelucire 50/13, the void diameters of the extrudates with the particulate additives are fairly consistent throughout the dissolution process. This indicates that a surface erosion process dominates the dissolution process. This is confirmed by the SEM results of the extrudates. As seen in **Figure 14**, after 2 hours of the dissolution, the surface of the extrudates with interior voids all show the full exposure of open voids at the surfaces. The cross-section images of the extrudates show little visible changes in comparison to the fresh samples (**Figure 1**). This is good evidence suggesting the surface erosion is the main mechanism of the dissolution process.

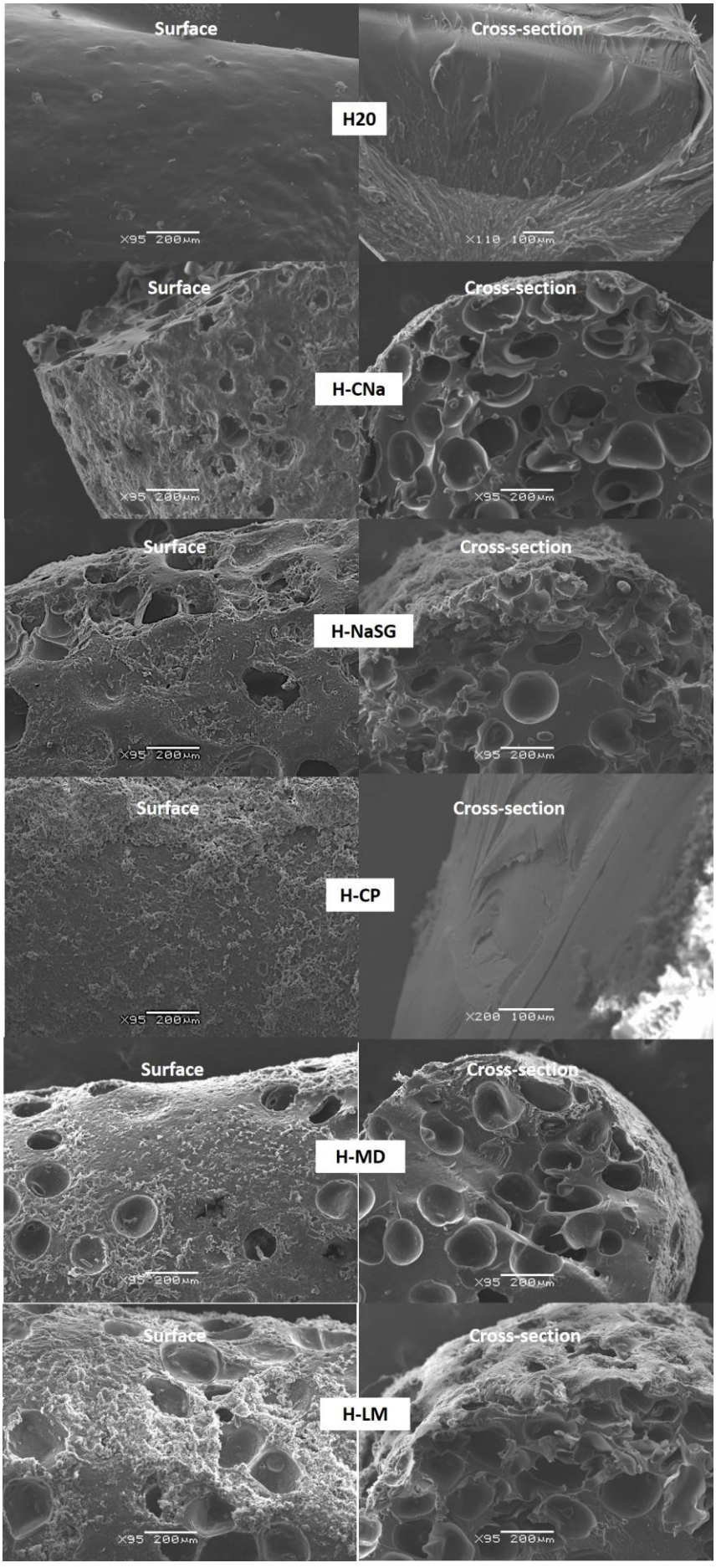
Surface
Cross-section
H20
X95 200µm
X110 100µm
Surface
Cross-section
H-CNa
X95 200µm
X95 200µm
Surface
Cross-section
H-NaSG
X95 200µm
X95 200µm
Surface
Cross-section
H-CP
X95 200µm
X200 100µm
Surface
Cross-section
H-MD
X95 200µm
X95 200µm
Surface
Cross-section
H-LM
X95 200µm
X95 200µm

Figure 14. SEM images of the surfaces and the cross sections of the extrudates after 2 hours of the dissolution tests in pH 6.8 PBS followed by drying (the crusty texture of the surfaces is a results of salt crystallisation of the dissolution media used during drying).

Conclusion

This study explored the origin of the void formation in HME extrudates primarily produced by lab scale hot melt extruders and investigated the factors that can be used to manipulate the size and number density of such voids. The results indicated that the viscosity and the presence of phase-separated particulates are essential for the formation of the voids. It is likely that the particulates act as nuclei for bubbles forming from entrapped air and, if they contain moisture, steam formed from the moisture released during processing. A threshold level of the viscosity of the mixture controls the collapse/escape of the bubbles. Therefore in order to minimise void formation, the results of this study indicate that low moisture content of the raw materials, low proportion of particulates and the addition of lubricants, such as low melting lipid excipients, could be beneficial. Slow screw speed is also preferred for reducing the formation of the voids. This study systematically reported the mechanism of void formation in HME extrudates and generated new insights into the strategies that can be used to manage such void formations.

Acknowledgments

This project has received funding from the Interreg 2 Seas programme 2014-2020 co-funded by the European Regional Development Fund under subsidy contract 2S01-059_IMODE. Johnson Matthey and the U.K. Engineering and Physical Sciences Research Council (EPSRC) are also acknowledged for the funding of the PhD project of Mohammed Al-Sharabi.

References:

ALMEIDA, A., POSSEMIERS, S., BOONE, M. N., DE BEER, T., QUINTEN, T., VAN HOOREBEKE, L., REMON, J. P. & VERVAET, C. 2011. Ethylene vinyl acetate as matrix for oral sustained release dosage forms produced via hot-melt extrusion. *European Journal of Pharmaceutics and Biopharmaceutics,* 77**,** 297-305.

ALQAHTANI, F., BELTON, P., WARD, A., ASARE-ADDO, K. & QI, S. 2020. An investigation into the use of low quantities of functional additives to control drug release from hot melt extruded solid dispersions for poorly soluble drug delivery. *International Journal of Pharmaceutics,* 579**,** 119172.

ALSHAFIEE, M., ALJAMMAL, M. K., MARKL, D., WARD, A., WALTON, K., BLUNT, L., KORDE, S., PAGIRE, S. K., KELLY, A. L., PARADKAR, A., CONWAY, B. R. & ASARE-ADDO, K. 2019. Hot-melt extrusion process impact on polymer choice of glyburide solid dispersions: The effect of wettability and dissolution. *International Journal of Pharmaceutics,* 559**,** 245-254.

BALOGH, A., DRÁVAVÖLGYI, G., FARAGÓ, K., FARKAS, A., VIGH, T., SÓTI, P. L., WAGNER, I., MADARÁSZ, J., PATAKI, H., MAROSI, G. & NAGY, Z. K. 2014. Plasticized Drug-Loaded Melt Electrospun Polymer Mats: Characterization, Thermal Degradation, and Release Kinetics. *Journal of Pharmaceutical Sciences,* 103**,** 1278-1287.

CALIANDRO, R., DI PROFIO, G. & NICOLOTTI, O. 2013. Multivariate analysis of quaternary carbamazepine–saccharin mixtures by X-ray diffraction and infrared spectroscopy. *Journal of Pharmaceutical and Biomedical Analysis,* 78-79**,** 269-279.

CROWLEY, M. M., SCHROEDER, B., FREDERSDORF, A., OBARA, S., TALARICO, M., KUCERA, S. & MCGINITY, J. W. 2004. Physicochemical properties and mechanism of drug release from ethyl cellulose matrix tablets prepared by direct compression and hot-melt extrusion. *International Journal of Pharmaceutics,* 269**,** 509-522.

DENG, W., MAJUMDAR, S., SINGH, A., SHAH, S., MOHAMMED, N. N., JO, S., PINTO, E., TEWARI, D., DURIG, T. & REPKA, M. A. 2013. Stabilization of fenofibrate in low molecular weight hydroxypropylcellulose matrices produced by hot-melt extrusion. *Drug Dev Ind Pharm,* 39**,** 290-8.

FUKUDA, M., PEPPAS, N. A. & MCGINITY, J. W. 2006. Floating hot-melt extruded tablets for gastroretentive controlled drug release system. *Journal of Controlled Release,* 115**,** 121-129.

GRZESIAK, A. L., LANG, M., KIM, K. & MATZGER, A. J. 2003. Comparison of the four anhydrous polymorphs of carbamazepine and the crystal structure of form I. *Journal of pharmaceutical sciences,* 92**,** 2260-2271.

GUPTA, S. S., MEENA, A., PARIKH, T. & SERAJUDDIN, A. T. 2016. Investigation of thermal and viscoelastic properties of polymers relevant to hot melt extrusion-I: Polyvinylpyrrolidone and related polymers. *Journal of Excipients and Food Chemicals,* 5**,** 1001.

HANN, D. B., CHERDANTSEV, A. V. & AZZOPARDI, B. J. 2018. Study of bubbles entrapped into a gas-sheared liquid film. *International Journal of Multiphase Flow,* 108**,** 181-201.

KRUPA, A., CANTIN, O., STRACH, B., WYSKA, E., TABOR, Z., SIEPMANN, J., WRÓBEL, A. & JACHOWICZ, R. 2017. In vitro and in vivo behavior of ground tadalafil hot-melt extrudates: How the carrier material can effectively assure rapid or controlled drug release. *International Journal of Pharmaceutics,* 528**,** 498-510.

LANDAU, L. & LIFSHITZ, E. 1987. Theoretical Physics, vol. 6, Fluid Mechanics. Pergamon, London.
MARTINEZ-MARCOS, L., LAMPROU, D. A., MCBURNEY, R. T. & HALBERT, G. W. 2016. A novel hot-melt extrusion formulation of albendazole for increasing dissolution properties. *International Journal of Pharmaceutics,* 499**,** 175-185.
MARU, S. M., DE MATAS, M., KELLY, A. & PARADKAR, A. 2011. Characterization of thermal and rheological properties of zidovidine, lamivudine and plasticizer blends with ethyl cellulose to assess their suitability for hot melt extrusion. *European Journal of Pharmaceutical Sciences,* 44**,** 471-478.
MEENA, A., PARIKH, T., GUPTA, S. S. & SERAJUDDIN, A. T. 2016. Investigation of thermal and viscoelastic properties of polymers relevant to hot melt extrusion-II: cellulosic polymers. *Journal of Excipients and Food Chemicals,* 5**,** 1002.
PARIKH, T., GUPTA, S. S., MEENA, A. & SERAJUDDIN, A. T. 2016. Investigation of thermal and viscoelastic properties of polymers relevant to hot melt extrusion-III: Polymethacrylates and polymethacrylic acid based polymers. *Journal of Excipients and Food Chemicals,* 5**,** 1003.
SADIA, M., ARAFAT, B., AHMED, W., FORBES, R. T. & ALHNAN, M. A. 2018. Channelled tablets: An innovative approach to accelerating drug release from 3D printed tablets. *Journal of Controlled Release,* 269**,** 355-363.
SADIA, M., SOŚNICKA, A., ARAFAT, B., ISREB, A., AHMED, W., KELARAKIS, A. & ALHNAN, M. A. 2016. Adaptation of pharmaceutical excipients to FDM 3D printing for the fabrication of patient-tailored immediate release tablets. *International journal of pharmaceutics,* 513**,** 659-668.
SMIRNOV, B. M. & BERRY, R. S. 2015. Growth of bubbles in liquid. *Chemistry Central Journal,* 9**,** 48.
SNEJDROVA, E. & DITTRICH, M. 2012. Pharmaceutical applications of plasticized polymers. *Recent advances in plasticizers,* 159**,** 23-34.
SOLANKI, N. G., GUMASTE, S. G., SHAH, A. V. & SERAJUDDIN, A. T. M. 2019. Effects of Surfactants on Itraconazole-Hydroxypropyl Methylcellulose Acetate Succinate Solid Dispersion Prepared by Hot Melt Extrusion. II: Rheological Analysis and Extrudability Testing. *Journal of Pharmaceutical Sciences,* 108**,** 3063-3073.